

Gravitating monopole and its black hole solution in Brans-Dicke Theory

Takashi Tamaki* and Kei-ichi Maeda†

Department of Physics, Waseda University, Shinjuku, Tokyo 169, Japan

Takashi Torii‡

Department of Physics, Tokyo Institute of Technology, Meguro, Tokyo 152, Japan

(September 9, 2018)

We find a self-gravitating monopole and its black hole solution in Brans-Dicke (BD) theory. We mainly discuss the properties of these solutions in the Einstein frame and compare the solutions with those in general relativity (GR) on the following points. : From the field distributions of the generic type of self-gravitating monopole solutions, we can find that the YM potential and the Higgs field hardly depend on the BD parameter for most of the solution. There is the upper limit of the vacuum expectation value of the Higgs field to exist a solution as in GR. Since the BD scalar field has the effect of lessening an effective gauge charge, the upper limit in BD theory (in the $\omega = 0$ case) becomes about 30% larger than in GR. In some parameter ranges, there are two nontrivial solutions with the same mass, one of which can be regarded as the excited state of the other. This is confirmed by the analysis by catastrophe theory, which stated that the excited solution is unstable. We also find that the BD scalar field varies larger for solutions of smaller horizon radius, which can be understood from the differences of non-trivial structure outside the horizon. A scalar mass and thermodynamical properties of new solutions are also examined. Our analysis may give an insight into solutions in other theories of gravity; particularly, a theory with a dilaton field may show similar effects because of its coupling to a gauge field.

04.70.-s, 04.50.+h, 95.30.Tg, 97.60.Lf.

I. INTRODUCTION

After the discovery of a particlelike solution in the Einstein-Yang-Mills (EYM) system by Bartnik and McKinnon [1], a variety of particlelike solutions and black hole solutions with non-Abelian fields were found [2–13]. Some of them are the solutions in which the self-gravity is taken into account for the solution in flat space-time. The others are new types of solutions which can exist in the presence of gravity. They show interesting properties, which can not be seen in the flat spacetime solutions or well known Kerr-Newman black hole, such as stability, thermodynamical properties, mass inflation phenomena and so on [14]. In the context of a counterexample for the black hole no-hair conjecture, a monopole black hole [9–13] may be the most important among them, since both the Reissner-Nordström (RN) black hole and the monopole black hole with the same mass and the gauge charge are stable within a certain parameter region and it is constructed in the EYM-Higgs (EYMH) system which is not a phenomenological model such as the Skyrme and the Proca model. The monopole black hole solution describes a space-time structure with an event horizon in the gravitating 't Hooft-Polyakov magnetic monopole [15]. The existence of such a black hole solution was first expected by examining a simple distribution of the energy density, where it is almost constant inside a core and decays as r^{-4} outside [9]. Later Breitenlohner *et al.* [11], Aichelburg [12] and we [13] found the “exact” solutions numerically.

In the big bang scenario, the 't Hooft-Polyakov monopole is overproduced during phase transitions in the early universe. This is one of the reasons why the inflationary scenario was proposed [16]. Although such an inflationary scenario was discussed originally in general relativity (GR), it turns out that introduction of a scalar field (such as the Brans-Dicke (BD) scalar field) can make a great change in scenarios of the very early universe [17]. Moreover, Vilenkin and Linde proposed that inflation occurs inside the 't Hooft-Polyakov monopole [18], where no fine tuning of the initial value is necessary. Such a monopole inflation is also changed qualitatively by introducing a scalar field [19]. So properties of the gravitating monopole and its black hole solution may be greatly modified in scalar-tensor theory compared with in GR.

*electronic mail: tamaki@gravity.phys.waseda.ac.jp

†electronic mail: maeda@gravity.phys.waseda.ac.jp

‡electronic mail: torii@th.phys.titech.ac.jp

As for the dilatonic black holes in an effective theory of superstring, it is known that such a scalar field also affects many features [20]. In BD theory, it is also known that the Kerr or Kerr-Newman black hole is a unique solution in the vacuum case or in the case with the Maxwell field, because of the conformal invariance of the Maxwell field and the black hole uniqueness theorem [21]. Recently, however, we found non-trivial black hole solutions with the non-Abelian field in BD theory [22]. They are generalizations of neutral non-Abelian black holes in GR (Proca [8] and Skyrme black holes [5]). Then, it is important to study a self-gravitating monopole and its black hole solution in BD theory as the charged solution. In addition, we have the following reasons to consider the monopole black hole in BD theory. (i) For the neutral non-Abelian black holes, we can not find a more stable solution than a trivial solution, i.e., Schwarzschild solution even in BD theory. We expect that the monopole black hole can be more stable than a trivial solution, i.e., Reissner-Nortström (RN) solution in the BD-YMH system. So it would be more important than the neutral type. Particularly, when we discuss the Hawking radiation [23] of the RN black hole in the EYMH system, it may evolve into the monopole black hole and eventually into the gravitating monopole, which would be a candidate for its remnant. The scalar field may cause a serious effect on this evolution. (ii) To investigate the stability of the neutral non-Abelian black holes, we can apply catastrophe theory even in BD theory [4,22]. Using the variables in the Einstein frame, we find that the BD scalar field is less important from the perspective of catastrophe theory. However the solution is not evident in the charged monopole black hole case.

This paper is organized as follows. We introduce basic *Ansätze* and the field equations in the BD-YMH system in Sec. II. In Sec. III, we present numerical solutions for the regular self-gravitating monopole. In order to see their structure, we show their field configurations and compare them with the solution in GR. We also discuss the upper limit of the vacuum expectation value of the Higgs field for a solution to exist. In Sec. IV, we present the monopole black hole solution. In some parameter regions, there exist two types of non-trivial solutions, one of which is stable and the other is not. We show that the dependence of field configurations on the BD parameter is different in each type. This shows the difference of the black hole structures which can not be seen only by considering them in GR. We also discuss upper limits for the vacuum expectation value of the Higgs field for a static solution to exist in black hole cases. The concluding remarks will follow in Sec. V. Throughout this paper we use units of $c=\hbar=1$. Notations and definitions follow Misner-Thorne-Wheeler [24].

II. BASIC EQUATIONS

The action of BD theory is written as [25]

$$S = \int d^4x \sqrt{-g} \left[\frac{1}{2\kappa^2} \left(\phi R - \frac{\omega}{\phi} \nabla_\alpha \phi \nabla^\alpha \phi \right) + L_m \right], \quad (2.1)$$

where $\kappa^2 \equiv 8\pi G$ with G being Newton's gravitational constant. ω is the BD parameter, and L_m is Lagrangian of the matter fields. The dimensionless BD scalar field ϕ is normalized by G . In our previous paper [22], we investigated two types of non-Abelian black hole solutions in BD theory (Proca black hole and Skyrme black hole) and found that there are several advantages to discussion in the Einstein conformal frame rather than in the BD frame. For example, the definition of thermodynamical variables of the solutions and the stability analysis using catastrophe theory. Although, of course, we can reach the same results in the BD frame, we transform the Einstein frame [26] as a matter of convenience. The conformal transformation in the present model is written by

$$\hat{g}_{ab} = \frac{\phi}{\phi_0} g_{ab}. \quad (2.2)$$

Then, we find the equivalent action $\hat{S} = S/\phi_0$ given as [27]

$$\hat{S} = \int d^4x \sqrt{-\hat{g}} \left[\frac{1}{2\kappa^2} \hat{R} - \frac{1}{2} \hat{\nabla}_\alpha \varphi \hat{\nabla}^\alpha \varphi + \frac{1}{\phi_0} \hat{L}_m \right], \quad (2.3)$$

where

$$\varphi \equiv \frac{1}{\kappa\beta} \ln \left(\frac{\phi}{\phi_0} \right), \quad (2.4)$$

$$\beta \equiv \left(\frac{2\omega + 3}{2} \right)^{-1/2}. \quad (2.5)$$

Variables with a caret $\hat{}$ denote those in the Einstein frame. \hat{L}_m is different from L_m unless the matter field is conformally invariant, as with the Yang-Mills field. The constant $\phi_0 \equiv 2(2+\omega)/(2\omega+3)$ is the value of the BD scalar field ϕ at spatial infinity, which guarantees that we can regard G as Newton's gravitational constant [25]. In this paper we investigate the YMH system, where Lagrangian \hat{L}_m is written as

$$\hat{L}_m = -\frac{1}{4}F_{\mu\nu}^a F^{\mu\nu a} - \frac{1}{2}e^{-\kappa\beta\varphi}(D_\mu\Phi^a)(D^\mu\Phi^a) - \frac{\lambda}{4}e^{-2\kappa\beta\varphi}(\Phi^a\Phi^a - v^2)^2 \quad (2.6)$$

$F_{\mu\nu}^a$ is the field strength of the SU(2) YM field and expressed by its potential A_μ^a as

$$F_{\mu\nu}^a = \partial_\mu A_\nu^a - \partial_\nu A_\mu^a + e\epsilon^{abc}A_\mu^b A_\nu^c, \quad (2.7)$$

with the gauge coupling constant e . Φ^a is the real triplet Higgs field and D_μ is the covariant derivative:

$$D_\mu\Phi^a = \partial_\mu\Phi^a + e\epsilon^{abc}A_\mu^b\Phi^c. \quad (2.8)$$

The theoretical parameters v and λ are the vacuum expectation value and the self-coupling constant of the Higgs field, respectively. Below we consider them only in the Einstein conformal frame, and drop the caret $\hat{}$.

We assume that a space-time is static and spherically symmetric, in which case the metric is written as

$$ds^2 = -\left[1 - \frac{2Gm(r)}{r}\right]e^{-2\delta(r)}dt^2 + \left[1 - \frac{2Gm(r)}{r}\right]^{-1}dr^2 + r^2d\Omega^2. \quad (2.9)$$

For the matter fields, we adopt the hedgehog ansatz given by

$$\Phi^a = vr^a h(r), \quad (2.10)$$

$$A_0^a = 0, \quad (2.11)$$

$$A_\mu^a = \omega_\mu^c \epsilon^{acb} \mathbf{r}^b \frac{1-w(r)}{er}, \quad (\mu = 1, 2, 3), \quad (2.12)$$

where \mathbf{r}^a and ω_μ^c are a unit radial vector in the internal space and a triad, respectively.

Variation of the action (2.3) with the matter Lagrangian (2.6) leads to the field equations

$$\frac{d\delta}{d\tilde{r}} = -\frac{8\pi\tilde{r}\tilde{v}^2\tilde{K}}{\phi_0}, \quad (2.13)$$

$$\frac{d\tilde{m}}{d\tilde{r}} = \frac{4\pi\tilde{r}^2\tilde{v}^2}{\phi_0} [f\tilde{K} + \tilde{U}], \quad (2.14)$$

$$\frac{d^2w}{d\tilde{r}^2} = \frac{1}{f} \left[\frac{1}{2} \frac{\partial\tilde{U}}{\partial w} + \frac{8\pi\tilde{r}\tilde{v}^2\tilde{U}}{\phi_0} \frac{dw}{d\tilde{r}} - \frac{2\tilde{m}}{\tilde{r}^2} \frac{dw}{d\tilde{r}} \right], \quad (2.15)$$

$$\frac{d^2h}{d\tilde{r}^2} = \frac{dh}{d\tilde{r}} \left(\beta \frac{d\tilde{\varphi}}{d\tilde{r}} - \frac{1}{\tilde{r}} \right) + \frac{1}{f} \left[e^{-\beta\tilde{\varphi}} \frac{\partial\tilde{U}}{\partial h} + \frac{8\pi\tilde{r}\tilde{v}^2\tilde{U}}{\phi_0} \frac{dh}{d\tilde{r}} - \frac{1}{\tilde{r}} \frac{dh}{d\tilde{r}} \right], \quad (2.16)$$

$$\frac{d^2\tilde{\varphi}}{d\tilde{r}^2} = -\frac{2}{\tilde{r}} \frac{d\tilde{\varphi}}{d\tilde{r}} - \frac{4\pi\beta\tilde{v}^2 e^{-\beta\tilde{\varphi}}}{\phi_0} \left(\frac{dh}{d\tilde{r}} \right)^2 + \frac{1}{f} \left[\frac{8\pi\tilde{v}^2}{\phi_0} \left(\frac{\partial\tilde{U}}{\partial\tilde{\varphi}} + \tilde{r}\tilde{U} \frac{d\tilde{\varphi}}{d\tilde{r}} \right) - \frac{2\tilde{m}}{\tilde{r}^2} \frac{d\tilde{\varphi}}{d\tilde{r}} \right], \quad (2.17)$$

where

$$f \equiv 1 - \frac{2\tilde{m}}{\tilde{r}}, \quad (2.18)$$

$$\tilde{U} \equiv \frac{(1-w^2)^2}{2\tilde{r}^4} + e^{-\beta\tilde{\varphi}} \left(\frac{wh}{\tilde{r}} \right)^2 + \frac{\tilde{\lambda}}{4} e^{-2\beta\tilde{\varphi}} (h^2 - 1)^2, \quad (2.19)$$

$$\tilde{K} \equiv \frac{1}{\tilde{r}^2} \left(\frac{dw}{d\tilde{r}} \right)^2 + \frac{e^{-\beta\tilde{\varphi}}}{2} \left(\frac{dh}{d\tilde{r}} \right)^2 + \frac{\phi_0}{16\pi\tilde{v}^2} \left(\frac{d\tilde{\varphi}}{d\tilde{r}} \right)^2. \quad (2.20)$$

We have introduced the following dimensionless variables:

$$\tilde{r} = evr, \quad \tilde{m} = Gevm, \quad \tilde{\varphi} = \kappa\varphi, \quad (2.21)$$

and dimensionless parameters:

$$\tilde{v} = v\sqrt{G}, \quad \tilde{\lambda} = \lambda/e^2. \quad (2.22)$$

Although the solution exists when $v \sim M_{Pl}$, where M_{Pl} is Planck mass, it can be described by a classical field configuration in the limit of a weak gauge coupling constant e , because its Compton wavelength $\sim e/v$ is much smaller than the radius of the classical monopole solution $\sim 1/ev$ in this case. Moreover, since the energy density $\sim e^2 v^4 \ll M_{Pl}^4$, we can treat the system classically.

The boundary conditions at spatial infinity are

$$\lim_{r \rightarrow \infty} m = M < \infty, \quad (2.23)$$

$$\lim_{r \rightarrow \infty} \delta = 0, \quad (2.24)$$

$$\lim_{r \rightarrow \infty} \kappa\beta\varphi = \lim_{r \rightarrow \infty} \ln \left(\frac{\phi}{\phi_0} \right) = 0, \quad (2.25)$$

$$\lim_{r \rightarrow \infty} h = 1, \quad (2.26)$$

$$\lim_{r \rightarrow \infty} w = 0. \quad (2.27)$$

These conditions imply that the space-time approaches a flat one and that the solution is a charged object. The field equations are singular at the origin and at the event horizon for a self-gravitating monopole and its black hole solution, respectively.

For a self-gravitating monopole solution, we require regularity at the origin. Expanding the Eqs. (2.13)-(2.17) around the origin, we find that regularity is guaranteed when the fields behaves as

$$w(\epsilon) \approx 1 + \frac{1}{2} C_w \epsilon^2 + O(\epsilon^3), \quad (2.28)$$

$$h(\epsilon) \approx C_h \epsilon + O(\epsilon^3), \quad (2.29)$$

$$\tilde{\varphi}(\epsilon) \approx C_\varphi - \frac{2\pi\beta}{\phi_0} e^{-\beta C_\varphi} \tilde{v}^2 \left(C_h^2 + \frac{\tilde{\lambda}}{3} e^{-\beta C_\varphi} \right) \epsilon^2 + O(\epsilon^3), \quad (2.30)$$

$$\delta(\epsilon) \approx C_\delta - \frac{4\pi\tilde{v}^2}{\phi_0} \left(C_w^2 + \frac{e^{-\beta C_\varphi}}{2} C_h^2 \right) \epsilon^2 + O(\epsilon^3), \quad (2.31)$$

$$\tilde{m}(\epsilon) \approx -\frac{2\pi\tilde{v}^2}{\phi_0} \left(C_w^2 + e^{-\beta C_\varphi} C_h^2 + \frac{\tilde{\lambda}}{6} e^{-2\beta C_\varphi} \right) \epsilon^3 + O(\epsilon^4). \quad (2.32)$$

C_w , C_h and C_φ are constant, which should be determined iteratively so that the boundary conditions (2.25)-(2.27) are satisfied. We also require that no singularity exists, i.e.,

$$m(r) < \frac{r}{2G}. \quad (2.33)$$

In the case of the monopole black hole, we assume the existence of a regular event horizon at $r = r_H$. For the metric

$$m_H \equiv m(r_H) = \frac{r_H}{2G}, \quad (2.34)$$

$$\delta_H \equiv \delta(r_H) < \infty. \quad (2.35)$$

For the matter fields, the square brackets in Eqs. (2.15)-(2.17) must vanish at the horizon. Hence we find that

$$\left. \frac{dw}{d\tilde{r}} \right|_{\tilde{r}=\tilde{r}_H} = \frac{w_H \phi_0}{F} (1 - w_H^2 - h_H^2 \tilde{r}_H^2 e^{-\beta \tilde{\varphi}_H}) \quad (2.36)$$

$$\left. \frac{dh}{d\tilde{r}} \right|_{\tilde{r}=\tilde{r}_H} = -\frac{h_H \phi_0}{F} [2w_H^2 + \tilde{\lambda} \tilde{r}_H^2 (h_H^2 - 1) e^{-\beta \tilde{\varphi}_H}] \quad (2.37)$$

$$\left. \frac{d\varphi}{d\tilde{r}} \right|_{\tilde{r}=\tilde{r}_H} = \frac{2\pi\beta\tilde{v}^2 e^{-\beta\tilde{\varphi}_H}}{F} [\tilde{\lambda} \tilde{r}_H^2 e^{-\beta\tilde{\varphi}_H} (h_H^2 - 1)^2 + 2w_H^2 h_H^2], \quad (2.38)$$

where

$$F = 2\pi\tilde{v}^2 \tilde{r}_H [2\tilde{r}_H^{-2} (1 - w_H^2)^2 + 4e^{-\beta\tilde{\varphi}_H} w_H^2 h_H^2 + \tilde{\lambda} \tilde{r}_H^2 (h_H^2 - 1)^2 e^{-2\beta\tilde{\varphi}_H}] - \phi_0 \tilde{r}_H. \quad (2.39)$$

We also require that no singularity exists outside the horizon, i.e.,

$$m(r) < \frac{r}{2G} \quad \text{for } r > r_H. \quad (2.40)$$

Hence, we should determine the values of C_w , C_h and C_φ (self-gravitating monopole case) or $\tilde{\varphi}_H$, w_H , and h_H (monopole black hole case) iteratively so that the boundary conditions at infinity are fulfilled. In this sense these are shooting parameters. It is a remarkable property of the nontrivial structure of many systems discussed before that we can not choose arbitrarily the values both of the fields and of their derivatives at the horizon. When we investigate the internal structure of non-Abelian black holes, we may expect the existence of the inner (Cauchy) horizon. There, the fields must satisfy the same type of constraint such as Eqs. (2.36)-(2.38). However, the shooting parameters on the black hole horizon which satisfy the boundary condition at infinity do not necessarily fulfill the constraint at the inner horizon. By this behavior the mass function diverges and a mass inflation phenomenon is realized inside of the black hole event horizon for non-Abelian black holes [14].

A non-trivial solution does not necessarily exist for the given theoretical parameters. However, for arbitrary values of \tilde{v} and $\tilde{\lambda}$, there exists a RN black hole solution such as

$$w = 0, \quad h = 1, \quad \delta = 0, \quad \phi = \phi_0, \quad \tilde{m}(\tilde{r}) = \tilde{M} - \frac{2\pi\tilde{v}^2}{\phi_0\tilde{r}}. \quad (2.41)$$

\tilde{M} is the gravitational mass at spatial infinity and $\tilde{Q} \equiv 2\tilde{v}\sqrt{\pi/\phi_0}$ is the magnetic charge of the black hole. The radius of the event horizon of the RN black hole is constrained to be $\tilde{r}_H \geq \tilde{Q}$. The equal sign case implies an extreme solution. If we equate $\beta = 0$, (i.e., $\omega \rightarrow \infty$) the model recovers the EYMH system and we find a self-gravitating monopole and its black hole solution investigated in Ref. [9–13]. In addition, if we put $G = 0$, i.e., neglect the gravitational effect, the model recovers the YMH system, which has a famous 't Hooft-Polyakov solution for a regular magnetic monopole [15]. Further, assuming $\lambda = 0$, we obtain the BPS monopole solution [28],

$$w(\tilde{r}) = \frac{\tilde{r}}{\sinh \tilde{r}}, \quad h(\tilde{r}) = \coth \tilde{r} - \frac{1}{\tilde{r}}. \quad (2.42)$$

In the next section, we show the solutions of a self-gravitating monopole both in GR and BD theory.

III. SELF-GRAVITATING MONOPOLE IN BRANS-DICKE THEORY

The self-gravitating monopole in GR were investigated in detail by several authors [9–13] and found to have many interesting properties, some of which can not be seen for the monopole solution in flat space-time. We list their properties. (1) The distribution of the non-Abelian structure decays exponentially with respect to the distance from the origin and the monopole has its core radius $\sim 1/ev$. (2) The solutions are characterized by the node number of the YM potential, which is different from topological winding number of the monopole. (3) There exists the maximum parameter v_{max} beyond which there is no monopole solution. v_{max} weakly depends on λ . (4) There exists the critical parameter $v_{extreme}$ for the small $\tilde{\lambda}$. At $v = v_{extreme}$, the monopole solution changes to extreme RN solution. Between $v_{extreme}$ and v_{max} , two monopole solutions with a different mass appear for each value of v . The higher mass solution is unstable while the lower one is stable. $v_{extreme}$ also weakly depends on λ .

Now we turn to the monopole solutions in BD theory and compare their properties with those in GR from the above points of view. Solving the system (2.13)-(2.20) with the boundary conditions (2.23)-(2.33), we obtain gravitating monopole solutions. Although they are found only numerically, there exists a rigorous proof of the existence of self-gravitating monopole and its black hole solution in the $\tilde{\lambda} \rightarrow \infty$ case in GR [11]. We expect that the same discussion holds in the more general case including BD theory.

We show the field configurations of the gravitating monopole in Figs. 1. We chose the parameters as $\tilde{v} = 0.1$, $\tilde{\lambda} = 0.1$ and several values of $\omega = -1.4, -1.0, 0, \infty$. The $\omega = \infty$ case corresponds to GR. (a) is \tilde{r} - h, w diagram. We can see that the configurations of the YM potential and the Higgs field hardly depend on the BD parameter ω . This implies that the solution can have almost the same structure as the 't Hooft-Polyakov monopole in flat space-time, where the repulsive force of the gauge field balances with the attractive force of the Higgs field. (b) and (c) are \tilde{r} - \tilde{m}_g and \tilde{r} - δ diagram, respectively. Since \tilde{m}_g is defined as

$$\tilde{m}_g \equiv \tilde{m} + \frac{2\pi\tilde{v}^2}{\phi_0\tilde{r}}, \quad (3.1)$$

it diverges at the origin. The mass function \tilde{m}_g strongly depends on ω . For a different BD parameter each solution has a different effective global gauge charge \tilde{Q} . For the small ω , the charge is small, i.e., the monopole in BD theory has a smaller charge than that in GR. Since there is a prefactor \tilde{Q} in the δ and \tilde{m} equations, it contributes directly to the behavior of the metric functions. There is another factor which may change the behavior of metric functions. It is the BD scalar field φ . However from Fig. 1 (d), $\tilde{\varphi} \lesssim 0.07$ even for $\omega = -1.4$, which implies the $e^{-\beta\tilde{\varphi}} \approx 1$. $d\tilde{\varphi}/d\tilde{r}$ term is also smaller than other terms in the field equations. Hence we can neglect the $\tilde{\varphi}$ contribution to other fields in the *zeroth* approximation. However, we may not neglect the $\tilde{\varphi}$ contribution for the parameter range $v \approx v_{extreme}$ discussed later, where the gravitational effect plays an important roll.

In Fig. 2 we show the distribution of the energy density $\rho \equiv -T_0^0$ for the same parameters as Fig. 1 (It is normalized as $\tilde{\rho} = \rho G/(ev)^2$). An arrow shows the core radius of the monopole. The prefactor $1/\phi_0$ for the matter Lagrangian can be absorbed by defining the new variables and the effective parameters as $\tilde{A}_\mu^a = A_\mu^a/\sqrt{\phi_0}$, $\tilde{\Phi} = \Phi/\sqrt{\phi_0}$, $\tilde{e} = \sqrt{\phi_0}e$, $\tilde{v} = v/\sqrt{\phi_0}$ and $\tilde{\lambda} = \phi_0\lambda$. Hence the core radius $\sim 1/\tilde{e}\tilde{v} = 1/ev$ hardly depends on ϕ_0 , i.e. BD parameter ω . The energy density is almost constant inside the monopole core, but it decays as $1/\tilde{r}^4$ outside. Note that although w decays exponentially, the YM potential decays $\sim 1/r$ for a large radius.

As for the monopole in flat space-time, the uniqueness of the solution was proven [29], which means there is no excited mode of this solution. As for gravitating counterpart, however, there exist radial excited solutions characterized by the node number n of the YM potential for small \tilde{v} in GR [11]. We also find such excited solutions in BD theory. In the $v \rightarrow 0$ limit, the Higgs field becomes constant and the YM field recovers its apparent gauge symmetry. Then the YM field is conformally invariant and the BD scalar field becomes trivial by the regularity. As a result, the $n = 1$ excited solution approaches a regular Bartnik-McKinnon solution [1] in the EYM system in this limit as discussed in Ref. [11]. Hereafter, we focus on the solution with $n = 0$, i.e., the ground state solution.

In GR, there is the maximum value of the vacuum expectation value \tilde{v}_{max} for a fixed $\tilde{\lambda}$ where a regular monopole solution can exist [11]. We can understand this intuitively as follows. We compare the mass of the monopole $\sim 4\pi v/e$ with its core radius $\sim 1/ev$. When v becomes large, the mass of the monopole increases, as does the gravitational radius $\sim 8\pi Gv/e$, while its core radius shrinks. Hence, its core radius eventually gets into gravitational radius and the solution may develop into the RN black hole being swallowed in its non-trivial structure by the horizon. The existence of the boundary of the parameter is interesting also in the context of the inflation. Since there is no non-trivial static configuration beyond the maximum parameter, the solution must take a configuration of the static RN black hole or a nonstatic configuration. One of the possibilities in the latter case is the inflating solution. Actually it is confirmed that the boundary of the static solution almost coincides with the parameter region where the monopole inflation occurs [18].

In BD theory, it was shown that when we consider the global monopole, any inflating monopole eventually shrinks contrary to the case in GR [19]. Although we consider gauge monopole here, the BD scalar field may give a serious effect. Moreover it is found that the gravitating monopole solution in $N = 4$ supersymmetric low-energy superstring theory exists for arbitrary values of vacuum expectation value of the Higgs field, where the dilatonic field plays an important role [30]. Since the BD scalar field can be regarded as the dilaton field in a special coupling constant case as can be seen in Eq. (2.3), there is a possibility that \tilde{v}_{max} disappears. Actually, taking \tilde{v} larger, we find the BD scalar field gives a larger contribution. Hence we are interested in examining the maximum value \tilde{v}_{max} in BD theory.

First, we discuss analytically the parameter region where the nontrivial solutions exist following the analysis in Ref. [9]. For the monopole solution, the mass function behaves as Eq. (2.32) around the origin by regularity. At spatial infinity, the solution approaches RN solution,

$$\tilde{m}(\tilde{r}) = \tilde{M} - \frac{2\pi\tilde{v}^2}{\phi_0\tilde{r}} + \dots \quad (3.2)$$

From this boundary condition, g^{rr} should have a minimum which corresponds to the maximum of the \tilde{m}/\tilde{r} . This occurs around $\tilde{r}_m \sim 4\pi\tilde{v}^2/\phi_0\tilde{M}$. For the monopole in flat space-time, we have

$$\tilde{M}_{flat} = \frac{4\pi\tilde{v}^2}{\phi_0}g(\tilde{\lambda}), \quad (3.3)$$

$g(\tilde{\lambda})$ takes values from 1 to 1.787 when $\tilde{\lambda}$ changes from 0 to ∞ . We assume $\tilde{M} \propto \tilde{v}^2$ even for the gravitating monopole in both theories. Under this assumption, $\tilde{r}_m \sim 1/g \sim 1$. So g^{rr} takes a minimum value of about $g^{rr} \sim 1 - 4\pi\tilde{v}^2/\phi_0$. When $\tilde{v} = \tilde{v}_{extreme} = \sqrt{\phi_0/4\pi}$, g^{rr} takes 0 and the degenerate horizon appears at $r = r_{extreme}$. Because the region $\tilde{r} < \tilde{r}_{extreme}$ is separated infinitely in geodesic distance from the outer region [31], the monopole structure could be thought to be confined in the region $\tilde{r} < \tilde{r}_{extreme}$ and the solution looks like a RN black hole with the horizon radius $r_{extreme}$. Naively $\tilde{v}_{extreme}$ gives the maximum value of \tilde{v} . As a result, we can expect that the critical value $\tilde{v}_{extreme}$ becomes large for the large ϕ_0 , i.e., the small value of ω .

Breitenlohner et al. confirmed the above discussion numerically in GR ($\phi_0 = 1$) and found the maximum value \tilde{v}_{max} for the fixed $\tilde{\lambda}$ by examining the minimum of g^{rr} [11]. Moreover they found the parameter region of $\tilde{\lambda}$ where $\tilde{v}_{extreme}$ is not the maximum value of \tilde{v} . In the parameter region $\tilde{v}_{extreme} < \tilde{v} < \tilde{v}_{max}$, there are two different nontrivial solutions with the same \tilde{v} which is not obvious in the above simple analysis. On \tilde{v} - \tilde{M} diagram, these solutions construct two solution branches divided by a cusp structure at $\tilde{v} = \tilde{v}_{max}$. The lower mass branch ends up with \tilde{v}_{max} and the higher mass branch is connected to the RN black hole branch at $\tilde{v} = \tilde{v}_{extreme}$. The cusp structure is important for the stability analysis by using catastrophe theory [13]. For the larger $\tilde{\lambda}$, \tilde{v}_{max} and \tilde{v}_{crit} coincide [33]. Since \tilde{v}_{max} takes a value very close to $\tilde{v}_{extreme}$, we search $\tilde{v}_{extreme}$ by the behavior of g^{rr} first and estimate \tilde{v}_{max} .

In the same manner, we examine \tilde{v}_{max} in BD theory with $\omega = 0$. Figs. 3 shows the field configurations of the monopole with $\tilde{\lambda} = 0.2$ and around the maximum parameter \tilde{v}_{max} ((a) \tilde{r} - g^{rr} (b) \tilde{r} - h , w). We can find that g^{rr} has the minimum around $\tilde{r} = \tilde{r}_{extreme} \sim 1.53$ and the minimum value decreases as \tilde{v} becomes larger. When \tilde{v} approaches \tilde{v}_{max} , the behavior of the YM potential and the Higgs field changes more rapidly near the $\tilde{r}_{extreme}$ and takes $w \approx 0$ and $h \approx 1$, i.e., the solution can be approximated by a RN black hole solution outside of $\tilde{r}_{extreme}$. When we have $\tilde{v}_{extreme}$, the horizon degenerates and the outer region becomes the extreme RN black hole. Since the gravitational effect becomes strong around this parameter region as seen from Fig. 3 (a), the amplitude of $\tilde{\varphi}$ and the dependence of w and h on the BD parameter can not be negligible. We show the \tilde{v}_{max} - $\tilde{\lambda}$ diagram with $\omega = 0$ and ∞ in Fig. 4 (the solid lines). Though \tilde{v}_{max} is larger compared to the estimation $\tilde{v}_{extreme} = \sqrt{\phi_0/4\pi} \sim 0.282$ (for GR), ~ 0.325 (for $\omega = 0$) due to the naive estimation, we can obtain the relevant dependence of \tilde{v}_{max} on ϕ_0 (or ω). If we take a more accurate value of r_m calculated numerically, we have the better estimation of $\tilde{v}_{extreme} \sim 0.369$ (for GR) and $\tilde{v}_{extreme} \sim 0.497$ (for $\omega = 0$) As we describe later, the similar phenomena can be seen in monopole black hole. These are also shown in this diagram by the dotted lines (In this diagram, $\tilde{r}_H = 0.4$).

IV. MONOPOLE BLACK HOLE IN BRANS-DICKE THEORY

The monopole black hole solution in GR has the following properties in addition to (1)-(2) of Sec.III. The number of the solutions depends on the parameters complicatedly, since another parameter, the horizon radius, is added in the black hole case. We show the schematic diagram of \tilde{v} - \tilde{r}_H for small $\tilde{\lambda}$ in Fig. 5 [39]. In the shadowed region, the nontrivial solution exists. The $\tilde{r}_H = 0$ axis corresponds to the regular monopole solution. (5) For a fixed value of $\tilde{r}_H < \tilde{r}_H^*$ (See Fig. 5), we find two characteristic values \tilde{v}_{max} and $\tilde{v}_{extreme}$. They are extensions of properties (3) and (4) in the regular monopole case discussed in the previous section. In the region (i) in Fig. 5 ($\tilde{v}_{extreme} < \tilde{v} < \tilde{v}_{max}$),

there are two nontrivial solutions with different mass. The solution branch with higher mass is connected to the extreme RN black hole solution in the \tilde{v} - \tilde{M} diagram although the horizon radius changes discontinuously. (6) The solution in the lower mass branch is stable while the higher one is unstable. (7) For a fixed value of $\tilde{v} < \tilde{v}^*$ (See Fig. 5), there are two characteristic values $\tilde{r}_{H,max}$ and $\tilde{r}_{H,RN}$. In the region (ii) in Fig. 5 ($\tilde{r}_{H,RN} < \tilde{r} < \tilde{r}_{H,max}$), there are two nontrivial solutions. The solution branch with lower entropy (smaller \tilde{r}_H) is connected to the RN black hole at $\tilde{r}_H = \tilde{r}_{H,RN}$. (8) The solution in the high entropy branch is stable while the lower one is unstable. (9) The regions (i) and (ii) disappear for $\tilde{\lambda} > \tilde{\lambda}_{crit}^{(i)} \sim 0.287$ and $\tilde{\lambda} > \tilde{\lambda}_{crit}^{(ii)} \sim 0.696$, respectively. (10) When we consider the thermodynamics of the monopole black hole, its temperature diverges in the minimum mass limit unlike the RN black hole. Through an evaporation process from a large RN black hole, the solution experiences the first and/or second order phase transitions.

We turn to the monopole black hole in BD theory. Solving the system (2.13)-(2.20) numerically with the boundary conditions (2.23)-(2.27) and (2.34)-(2.40), we obtain a black hole solution. Figs. 6 are the field configurations with the parameters $\tilde{\lambda} = 0.1$, $\tilde{v} = 0.1$, $\omega = 0$ and the horizon radius $\tilde{r}_H = 0.2, 0.4$ and 0.6 ((a) \tilde{r} - h, w (b) \tilde{r} - \tilde{m}_g (c) \tilde{r} - δ (d) \tilde{r} - $\tilde{\varphi}$). We also plot the gravitating monopole solution, i.e., $\tilde{r}_H = 0$, for comparison. As the horizon radius becomes large, the curvature of the space-time outside the horizon would become small resulting in the variation of the BD scalar field being small. Hence the difference between the solutions in BD theory and in GR appears most conspicuously in the monopole solution case. The boundary value of w and h approaches $w(r_H) \rightarrow 0$ and $h(r_H) \rightarrow 1$ for a large horizon radius. Finally the solution becomes a RN black hole in the $\tilde{r}_H = \tilde{r}_{H,RN}$ limit. The behaviors of the solutions around this limit depend on the parameters complicatedly as discussed later.

In Fig.7(a), we show the \tilde{M} - \tilde{r}_H diagram for $\tilde{\lambda} = 0.1$, $\tilde{v} = 0.1$ and $\omega = -1.4, -1, 0$ and ∞ . Dotted lines show RN solution branches. Note that the RN solution in BD theory is different from that in GR because it has a different effective gauge charge by the factor ϕ_0 . Unlike the RN black hole, the monopole black hole does not have an extreme limit but has the $\tilde{r}_H = 0$ limit, which corresponds to the gravitating monopole solution. Fig.7(b) is a magnification around the maximum horizon radius of each theory. As is the case of GR, there are two solutions in some ranges of horizon radius. This parameter region corresponds to the region (ii) in Fig. 5. We call the upper (lower) branch a high (low) entropy branch. In both theories, these branches form a cusp structure at the point A , where the solution has the maximum horizon radius $\tilde{r}_{H,max}$. At the point B , the solution coincides with the RN black hole solution with the horizon radius $\tilde{r}_{H,RN}$. The solutions have a qualitatively similar structure in both theories. The maximum mass and the maximum horizon radius decrease when ω becomes small. Furthermore we find that the range of horizon radius where the low entropy branch exists becomes larger when we take the ω as small. These behaviors are mainly due to the effect of the boundary value of ϕ_0 . As we mentioned, $\tilde{v} = \tilde{v}/\sqrt{\phi_0}$ can be considered as an effective vacuum expectation value in BD theory. Since it becomes small when ω becomes small, we find that the width of region (ii) in Fig. 5 becomes large.

Next we consider a difference of solution in each branch. We consider the solution with $\tilde{v} = 0.1$, $\tilde{\lambda} = 0.1$ and $\tilde{r}_h = 0.59$, and change the BD parameter ω . Figs. 8 and 9 show configurations of the fields ((a) \tilde{r} - h, w (b) \tilde{r} - \tilde{m}_g (c) \tilde{r} - $\tilde{\varphi}$). In the high entropy branch (Fig. 9), the YM potential and the Higgs field hardly depend on ω . This is the same as the self-gravitating monopole case and the structure is supported by the balance between these fields. On the other hand, they have small amplitude in the low entropy branch (Fig. 10). The Higgs field can be approximated as $h \approx 1$, which means that it takes almost its vacuum value, while $w \approx 0$, where the YM potential decays as \tilde{r}^{-1} . Hence, what attracts the YM field is not the Higgs field but the self-gravitational attractive force. Actually, the counterpart of the low entropy branch does not exist in flat space-time. The dependence on ω in the low entropy branch is due to the difference of the effective gauge charge again. The horizon radius $\tilde{r}_h = 0.59$ line crosses the low entropy branch relatively near the point A (See Fig.8(b)). In the large ω (GR), however, it crosses around the point B , where the solution coincides with the RN black hole. Hence the field configurations approach a trivial solution.

In the present model, the YM field obtains the mass through a spontaneous symmetry breaking mechanism and the trace part of the energy-momentum tensor does not vanish. In this case the BD scalar field takes a nontrivial configuration and we can define the scalar mass M_s by the asymptotic behavior of the BD scalar field as

$$\phi \sim \phi_0 \left(1 + \frac{2GM_s}{r} \right). \quad (4.1)$$

Fig. 10 shows ω dependence of the gravitational mass M and scalar mass M_s for fixed horizon radius $\tilde{r}_h = 0.59$. As the solution can be approximated by the RN black hole in the zeroth approximation, M behaves as

$$\tilde{M} \approx \frac{1}{2\tilde{r}_h} \left[\tilde{r}_h^2 + 4\pi\tilde{v}^2 - \frac{2\pi\tilde{v}^2}{\omega + 2} \right]. \quad (4.2)$$

This gives good agreement with the ω dependence in Fig. 10(a). \tilde{M}_s can be expressed as [42]

$$\tilde{M}_s = \frac{1-2s}{2\omega+3}\tilde{M}, \quad (4.3)$$

where s is the sensitivity of a self-gravitating object. Though s varies as ω changes, its configuration is negligible for large ω and \tilde{M}_s behaves as $\sim 1/\omega$. Since $s \rightarrow 1/2$ in the $\omega \rightarrow -3/2$ limit, the fraction in Eq. (4.3) is indeterminate. However, Fig. 11(b) shows that \tilde{M}_s takes a non-zero finite value. As \tilde{M} takes almost the same value in each branch, the solution in the high entropy branch has smaller sensitivity than the lower branch.

In GR, it is considered that when λ becomes large, the parameter point where the $\tilde{r}_{H,RN} = \tilde{r}_{H,max}$ in Fig. 5s shifts to the left side, i.e., smaller \tilde{v} and the region (ii) becomes small. When $\tilde{\lambda}$ takes the critical value $\tilde{\lambda}_{crit}^{(ii)}$, the region (ii) finally disappears [11,4]. Although we do not examine the definite value of $\tilde{\lambda}_{crit}^{(ii)}$ in BD theory, the dependence on ω would be small because $\tilde{\lambda} = \lambda/e^2 = \bar{\lambda}/\bar{e}^2$ does not depend on ϕ_0 .

The stability of these exotic objects is one of the main interests. Aichelburg [12] analyzed the monopole black hole and its stability via the linear perturbation method in GR and showed that most of the solutions are stable within the limit of $\tilde{\lambda} \rightarrow \infty$. They also obtained the solutions in the finite $\tilde{\lambda}$ case and suggested that if we have two monopole black hole solutions for a fixed value of \tilde{v} , the low energy one is stable while the other is not. Similar works are found in [11], where the authors considered the weak coupling limit. We examined stabilities via catastrophe theory [13] and obtained a unified picture of the stabilities of the gravitating monopole and the monopole black hole. In catastrophe theory [40], we discuss the shape of a potential function as the variation of the control parameters. In that paper, we adopted $\tilde{\lambda}$, \tilde{v} and \tilde{M} as the control parameters, entropy S as the potential function and $\delta(r_h)$ as the state variable, and found that the system is classified into a swallow tail catastrophe. In general, a swallow tail catastrophe has three control parameters a , b , c and one state variable x and its potential function is described as

$$V = \frac{1}{5}x^5 + \frac{1}{3}ax^3 + \frac{1}{2}bx^2 + cx. \quad (4.4)$$

We regard the parameters as

$$a = a(\tilde{\lambda}, \tilde{v}), \quad b = b(\tilde{M}, \tilde{v}), \quad c = 0. \quad (4.5)$$

$\tilde{\lambda}_{crit}^{(ii)}$ is obtained by $a(\tilde{\lambda}_{crit}^{(ii)}, 0) = 0$. Although we have a new control parameter ω in BD theory, the situation does not change. By analyzing the dependence of the solution on the parameters, Eq. (4.5) is changed to

$$a = a(\tilde{\lambda}, \tilde{v}, \omega), \quad b = b(\tilde{M}, \tilde{v}, \omega), \quad c = 0, \quad (4.6)$$

i.e., the BD parameter is not an intrinsic parameter but a dummy parameter in catastrophe theory, and does not result in qualitative difference from GR. This is the same as in the neutral type non-Abelian black hole case [22]. As a result, the monopole black hole in BD theory is also classified as a swallow tail catastrophe. From this we find that the solution in the high entropy branch and RN black hole with larger horizon radius than $\tilde{r}_{H,RN}$ are stable, while the solutions in the low entropy branch and RN black hole with smaller horizon radius than $\tilde{r}_{H,RN}$ are unstable.

These properties are interesting in the context of black hole no-hair conjecture and the uniqueness of the solution. For $\tilde{\lambda} > \tilde{\lambda}_{crit}^{(ii)}$, there are two solutions (monopole black hole and RN black hole) when we fix the global charge M and Q . This is the counterexample of the strong no-hair conjecture, i.e., if the global charges are fixed, there exists only one solution. Moreover when $\tilde{\lambda}$ is smaller than $\tilde{\lambda}_{crit}^{(ii)}$, there is a mass range where two stable solutions (monopole black hole in the high entropy branch and RN black hole) exist for a fixed mass. This violates even the weak no-hair conjecture which states that if the global charges are fixed, there exists only one *stable* solution. These behaviors are shared by both theories. In GR, however, we have no idea how to identify whether a black hole is a monopole black hole or RN black hole from infinity, because the NA structure and the Higgs field decrease exponentially. On the other hand, in BD theory we can obtain the information about the scalar mass, which can be used to tell the type of black holes. Hence we can identify each black hole uniquely from infinity.

When we take into account the quantum effect, a black hole loses its energy by the Hawking evaporation process. The evolution of the monopole black hole by this process is rather complicated. First, we show an inverse temperature in the $\tilde{\lambda} = 1.0$, $\tilde{v} = 0.1$ and $\omega = 0, \infty$ (GR) in Fig. 11(a). The inverse temperature of the RN black hole has the minimum $1/T = 6\sqrt{3}\pi Q$ at $\tilde{M} = 2\tilde{Q}/\sqrt{3}$ and diverges at the extreme limit $\tilde{M} = \tilde{Q}$, where the evaporation ends. On the other hand, the inverse temperature of the monopole black hole becomes zero in the $\tilde{M} = \tilde{M}_{monopole}$ limit as with the Schwarzschild black hole. Consider the evolution of a RN black hole with $\tilde{r}_H > \tilde{r}_{H,max}$ by evaporation process. In GR in this figure, it loses mass, and when the solution approaches the minimum of the inverse temperature, its heat capacity changes discontinuously. [Note that its specific heat changes its sign continuously.] This is the second order phase transition. The black hole loses its mass further and reaches the point B . Below this mass, a RN black hole

becomes unstable and the solution traces the monopole black hole branch. The nontrivial structure comes out of the event horizon gradually. This is also the second phase transition. At this point, however, both the heat capacity and the specific heat change discontinuously. After that, the evaporation continues until the event horizon disappears. Finally, the regular monopole may remain as a remnant. For $\omega = 0$, however, it experiences a different evolution, because before it reaches the minimum of the inverse temperature, it reaches the point B and traces the monopole black hole branch continuously.

Furthermore, the $\tilde{\lambda} < \tilde{\lambda}_{crit}^{(ii)}$ case is different. Fig. 11(b) shows the inverse temperature of the solutions with the $\tilde{\lambda} = 0.1$, $\tilde{v} = 0.1$. In the $\omega = -1.4, -1.0$ and 0 case, the RN black hole evolves to the point B as in the above case. However, since the RN black hole becomes unstable, the solution jumps to the stable monopole branch, increasing its entropy and temperature discontinuously (arrows in Fig. 11(b)). This is the first order phase transition. The nontrivial structure comes out suddenly (or catastrophically) from the horizon. In the $\omega = \infty$ case, the solution experiences the second order phase transition at $\tilde{M} = 2\tilde{Q}/\sqrt{3}$ before the first order phase transition. As shown above, the type and number of the phase transitions depend on the physical parameters. This property is more important for the stability of the solution in the system surrounded by a heat bath. In that system, stability change occurs at the point where the heat capacity diverges [41]. Another thing that we should note is that the monopole black hole objects are forced to be produced by this process if the accretion to the black hole is very little.

Until now, we have studied the solution in the rather small value of \tilde{v} corresponding to the left side of Fig. 5. and found the region (ii) in BD theory. Next we consider the \tilde{v}_{max} in BD theory. By the same method in the gravitating monopole case, we found \tilde{v}_{max} . Fig. 4 shows the existence region of the black hole solution ($\tilde{r}_H = 0.4$) in \tilde{v} - $\tilde{\lambda}$ plane for $\omega = 0$ and ∞ . In the left region of each dotted line, there are black hole solutions. When we take $\tilde{\lambda}$ as larger, the dependence of \tilde{v}_{max} becomes smaller. We can not see the intrinsic difference also in this diagram. It is different to clarify the detailed structure of region (i) in BD theory because of the fine tuning of the asymptotic value of the BD field. In GR the region (i) disappears at $\tilde{\lambda} = \tilde{\lambda}_{crit}^{(i)} \sim 0.287$. As discussed before, since $\tilde{\lambda}$ does not depend on ϕ_0 , $\tilde{\lambda}^{(i)}$ would not be changed much even in BD theory. However, since the gravitational effect becomes strong around $\tilde{v} = \tilde{v}_{max}$, the BD scalar field may affect the value of $\tilde{\lambda}_{crit}^{(i)}$. It needs further analysis to say definite thing.

V. CONCLUSION

We found the self-gravitating monopole and its black hole solution of monopole in BD theory and compared them with those in GR. We clarified the following important aspects. The configuration of the YM potential and the Higgs fields of a self-gravitating monopole and a monopole black hole hardly depend on the BD parameter in most of the mass range, which shows the structure resembles the 't Hooft-Polyakov monopole. We found the parameter region (ii) in Fig. 5, where two monopole black hole solutions exist for fixed horizon radius. Each solution branch has a different dependence for the BD parameter. For the higher entropy branch, the configurations of the fields hardly depend on the BD parameter, while the configuration of the fields changes to those of RN black hole in the $\tilde{v} \rightarrow \tilde{v}_{max}$ limit for the lower entropy branch. However, we can not find the region (i) because fine tuning is needed to satisfy the boundary condition of the BD field at infinity. One of the characteristic properties in BD theory is lessening the effective global gauge charge. By this effect, the \tilde{M} - \tilde{r}_h diagram (Fig. 7) shifts to the left side, i.e., the mass of the solution becomes small when ω gets small. From this diagram, we can derive information about stability by applying catastrophe theory. As in the GR case, the high (low) entropy branch is stable (unstable). And we found that the BD parameter is not an intrinsic parameter but a dummy parameter in catastrophe theory. The effective global charge also affects the configuration for the high entropy branch, and does affect the existence region of the solutions in parameter regions. We investigated a boundary value of \tilde{v} above which there exist no static solution for $\tilde{r}_h = 0.4$ and a self-gravitating solution. It is interesting that the allowed parameter region is extended in BD theory. We also discuss the thermodynamical properties of the black hole solutions. The number and the order of the phase transitions depend complicatedly on the theoretical parameters.

These aspects may give us some important information about monopole black holes in other theories of gravity. In particular, we can anticipate the results in dilaton gravity because of its similarity to BD theory. Though we can not see the intrinsic qualitative difference from GR, some effective theory of unified theory may cause important effects for monopole [30] or its black hole solution, which may predict some information to the remnant of the Hawking evaporation.

There are some issues which we should comment on. In this paper, we transformed the system from the original BD frame to the Einstein frame and discussed only in the latter frame. However, the solutions in the former frame are easily obtained from our solution by the inverse transformation of Eq. (2.2). For example, M - r_H diagram in the BD frame is obtained as follows. In the BD frame, a gravitational mass M_{BD} is defined by use of the scalar mass as

[42]

$$M_{BD} = M + M_s . \quad (5.1)$$

The $\tilde{M}_{BD}-\tilde{r}_H$ diagram is shown in Fig. 12, where we normalize as $\tilde{M}_{BD} = GevM_{BD}$. Because of the existence of a scalar field, a cusp structure disappears at the points A . This may show that \tilde{M}_{BD} is not appropriate to a control parameter of catastrophe theory [22,44]. Since the solution in a high entropy branch has a larger scalar mass than that in a low entropy branch as shown in Fig. 10, the high entropy branch slides to the right of the lower branch in the BD frame.

We note the relation between our results and other topological defects such as a global monopole or a cosmic string in BD theory or in more general scalar-tensor theories. For global monopole, it is investigated that a massless dilaton field or the BD scalar field affects its structure, and is discussed that there is no solution except the special value of the coupling constant [35]. Similar arguments are seen for a cosmic string in [36] where they discussed that “wire approximation” which can be valid in GR will not be used. For a massive dilaton field, though both global monopole and cosmic strings would not be affected seriously compared to the massless case, it is discussed that it enables us to decide the dilaton mass from observation [37]. As for the texture, though exact results are almost unknown but Dando using self-similar ansatz showed that regular solution exists even in a massless dilaton case for a suitable choice of coupling constant [38]. Contrary to these cases, both the self-gravitating monopole and its black hole solution exist for any value of the BD parameter in our model. This would be due to the asymptotic mild behavior of the BD scalar field.

We finally note that much work on the monopole solution has been developing from the context of superstring theory [45]. Recently monopole solutions in flat space-time, self-gravitating monopole solutions and its black hole solutions were obtained in Born-Infeld type action [46]. However, little has been clarified about them. It should be interesting to investigate their structure, especially the internal structure around the central singularity, because of the remarkable form of its action.

ACKNOWLEDGEMENTS

We would like to thank J. Koga and T. Tachizawa for useful discussions. (T. T.)² are thankful for financial support from the JSPS. This work was supported partially by a Grant-in-Aid for Scientific Research Fund of the Ministry of Education, Science and Culture (Specially Promoted Research No. 08102010 and No. 09410217), by a JSPS Grant-in-Aid (No. 094162), and by the Waseda University Grant for Special Research Projects.

-
- [1] R. Bartnik and J. Mckinnon, Phys. Rev. Lett. **61**, 141 (1988).
 - [2] As a review paper see K. Maeda, Journal of the Korean Phys. Soc. **28**, S468, (1995), and M. S. Volkov and D. V. Gal'tsov, hep-th/9810070.
 - [3] M. S. Volkov and D. V. Galt'sov, Pis'ma Zh. Eksp. Theor. Fiz. **50**, 312 (1989); P. Bizon, Phys. Rev. Lett. **64**, 2844 (1990); H. P. Künzle and A. K. Masoud-ul-Alam, J. Math. Phys. **31**, 928 (1990).
 - [4] K. Maeda, T. Tachizawa, T. Torii and T. Maki, Phys. Rev. Lett. **72**, 450 (1994); T. Torii, K. Maeda and T. Tachizawa, Phys. Rev. D. **51**, 1510 (1995).
 - [5] S. Droz, M. Heusler and N. Straumann, Phys. Lett. B **268**, 371 (1991); P. Bizon and T. Chmaj, Phys. Lett. B **297**, 55 (1992).
 - [6] H. Luckock and I. G. Moss, Phys. Lett. B **176**, 341 (1986); H. Luckock, in *String theory, quantum cosmology and quantum gravity, integrable and conformal invariant theories*, eds. H. de Vega and N. Sanchez, (World Scientific, Singapore, 1986), p. 455.
 - [7] T. Torii and K. Maeda, Phys. Rev. D **48**, 1643 (1993).
 - [8] B. R. Greene, S. D. Mathur and C. M. O'Neill, Phys. Rev. D **47**, 2242 (1993).
 - [9] K. -Y. Lee, V. P. Nair and E. Weinberg, Phys. Rev. Lett. **68**, 1100 (1992); Phys. Rev. D **45**, 2751 (1992); Gen. Relativ. Gravit. **24**, 1203 (1992)
 - [10] M. E. Ortiz, Phys. Rev. D. **45**, R2586 (1992).
 - [11] P. Breitenlohner, P. Forgács and D. Maison, Nucl. Phys. B **383**, 357 (1992); *ibid.* **442**, 126 (1995).
 - [12] P. C. Aichelberg and P. Bizon, Phys. Rev. D. **48**, 607 (1993).
 - [13] T. Tachizawa, K. Maeda and T. Torii, Phys. Rev. D. **51**, 4054 (1995).

- [14] E. E. Donets, D. V. Gal'tsov and M. Yu. Zotov, Phys. Rev. D **56**, 3459 (1997); *ibid.*, Pis'ma Zh. Eksp. Teor. Fiz., **65**, 855 (1997); P. Breitenlohner, G. Lavrelashvili and D. Maison, Nucl. Phys. B **524**, 427 (1998).
- [15] G. 't Hooft, Nucl. Phys. B **79**, 276 (1974); A. M. Polyakov, Pis'ma Zh. Eksp. Teor. Fiz. **20**, 430 (1974) [JETP Lett. **20**, 194 (1974)].
- [16] A. H. Guth, Phys. Rev. D **23**, 347 (1981); J. R. Gott, Nature (London) **295**, 304 (1982); K. Sato, H. Kodama, M. Sasaki and K. Maeda, Phys. Lett. B **108**, 35 (1982).
- [17] D. La and P.J. Steinhardt, Phys. Rev. Lett. **62**, 376 (1989); A.L. Berkin, K. Maeda and J. Yokoyama, *ibid.* **65**, 141 (1990); A.L. Berkin and K. Maeda, Phys. Rev. D **44**, 1691 (1991); A. D. Linde, *ibid.* **49**, 748 (1994); J. Garcia-Bellido, A. D. Linde and D. A. Linde, *ibid.* **50**, 730 (1994).
- [18] A. Vilenkin, Phys. Rev. Lett. **72**, 3137 (1994); A. D. Linde, Phys. Lett. B **327**, 208 (1994); N. Sakai, H. Shinkai, T. Tachizawa and K. Maeda, Phys. Rev. D **53**, 655 (1996); N. Sakai, *ibid.* **54**, 1548 (1996); I. Cho and A. Vilenkin, *ibid.* **56**, 7621 (1997).
- [19] N. Sakai, J. Yokoyama and K. Maeda, Phys. Rev. D **59**, 103504 (1999).
- [20] G.W. Gibbons and K. Maeda, Nucl. Phys. B **298**, 741 (1988).
- [21] J.D.Bekenstein, Phys. Rev. D **5**, 1239 (1972); S. W. Hawking, Comm. Math. Phys. **25**, 167 (1972).
- [22] T. Tamaki, K. Maeda and T. Torii, Phys. Rev. D **57**, 4870 (1998).
- [23] S. W. Hawking, Nature **248**, 30 (1974); Commun. Math. Phys. **43**, 199 (1975).
- [24] C. W. Misner, K. S. Thorne and J. A. Wheeler, *Gravitation* (Freeman, New York 1973).
- [25] C. Brans and R. H. Dicke, Phys. Rev. **124**, 925 (1961).
- [26] R. H. Dicke, Phys. Rev. **125**, 2163 (1962).
- [27] Although singular solutions in the two conformal frames are not necessarily equivalent owing to the possibility of a singularity residing in the conformal rescaling (scalar field), solutions will map onto each other provided that they have a regular horizon and are asymptotically flat, which we assume here.
- [28] M. K. Prasad and C. M. Sommerfield, Phys. Rev. Lett. **35**, 760 (1975).
- [29] D. Maison, Nucl. Phys. B. **182**, 144 (1981).
- [30] J. A. Harvey and J. Liu, Phys. Lett. B **268**, 40 (1991).
- [31] Similar phenomena can be seen in the cosmic string. There exist string solution and the Melvin solution under some value of v . As v gets larger, both solution approaches each other. When it reaches critical value for which the deficit angle becomes 2π , there exists only cylindrical solution [32].
- [32] M. Christensen, A. L. Larsen and Y. Verbin, gr-qc/9904049.
- [33] For the very large value of λ , it is discussed in [34] that there appears a second minimum for g^{rr} inside a first minimum near the $\tilde{v}_{extreme}$. As \tilde{v} increase, the outer minimum moves upward, while the inner minimum downward.
- [34] A. Lue and E. J. Weinberg, hep-th/9905223.
- [35] A. Barros and C. Romero, Phys. Rev. D **56**, 6688 (1997); A. Banerjee, A. Beesham, S. Chatterjee and A. A. Sen, Class. Quantum Grav. **15**, 645 (1998); O. Dando and R. Gregory, Class. Quantum Grav. **15**, 985 (1998).
- [36] C. Gundlach and M. E. Ortiz, Phys. Rev. D **42**, 2521 (1990); A. Barros and C. Romero, J. Math. Phys. **36**, 5800 (1995); A. A. Sen, N. Banerjee and A. Banerjee, Phys. Rev. D **56**, 3706 (1997); M. Emilia and X. Guimarães, Class. Quantum Grav. **14**, 435 (1997).
- [37] T. Damour and A. Vilenkin, Phys. Rev. Lett. **78**, 2288 (1997); R. Gregory and C. Santos, Phys. Rev. D **56**, 1194 (1997).
- [38] O. Dando, gr-qc/9904058.
- [39] The precise diagram is given in Ref. [11].
- [40] T. Poston and I. Stewart, *Catastrophe Theory and Its Applications*, Pitman, London (1978); R. Thom, *Structure Stability and Morphogenesis*, Benjamin (1975).
- [41] J. Katz, I. Okamoto and O. Kaburaki, Class. Quantum Grav. **10**, 1323 (1993).
- [42] C. Will, *Theory and experiment in gravitational physics*, (Cambridge university press, Cambridge 1981).
- [43] It was shown that gravitational mass in the Einstein frame satisfy the first law of black hole thermodynamics [44].
- [44] J. Koga and K. Maeda, Phys. Rev. D **58** 064020 (1998).
- [45] C. G. Callan and J. M. Maldacena, Nucl. Phys. B **513**, 198 (1998); G. Gibbons, Nucl. Phys. B **514**, 603 (1998).
- [46] N. Grandi, E. F. Moreno and F. A. Schaposnik, hep-th/9901073; P. K. Tripathy, hep-th/9904186.

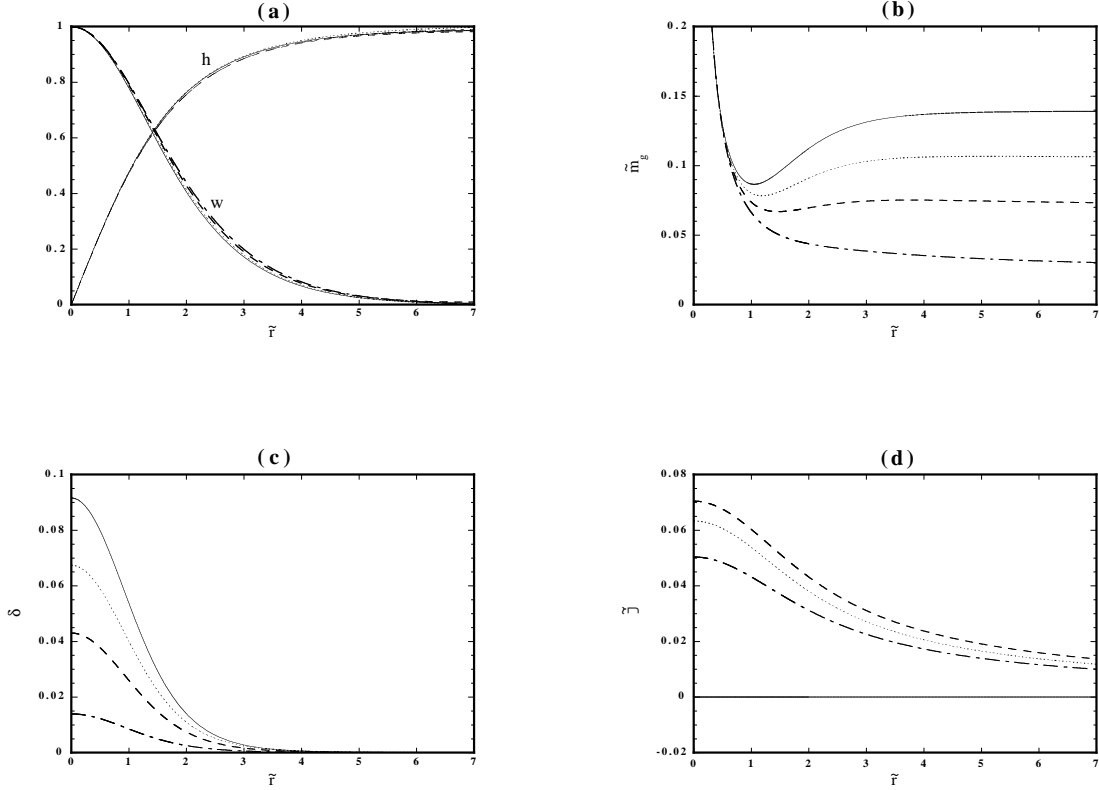


FIG. 1. Field configurations of the self-gravitating monopole for $\tilde{v} = 0.1$ and $\tilde{\lambda} = 0.1$ ((a) \tilde{r} - h, w (b) \tilde{r} - \tilde{m}_g (c) \tilde{r} - δ (d) \tilde{r} - $\tilde{\varphi}$). We compared these distributions for $\omega = -1.4, -1, 0, \infty$. Though metric functions and the scalar field depend on the BD parameter mainly due to the difference of the effective global charge, we can find that YM field and the Higgs field hardly do.

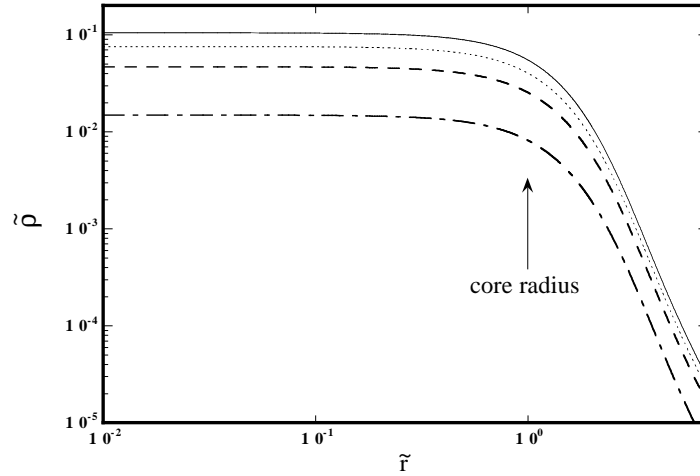


FIG. 2. The density distribution of the monopole solution for the same parameters as Fig. 1. An arrow shows the core radius of the monopole which hardly depends on the BD parameter. The energy density decays as $1/\tilde{r}^4$ outside the core.

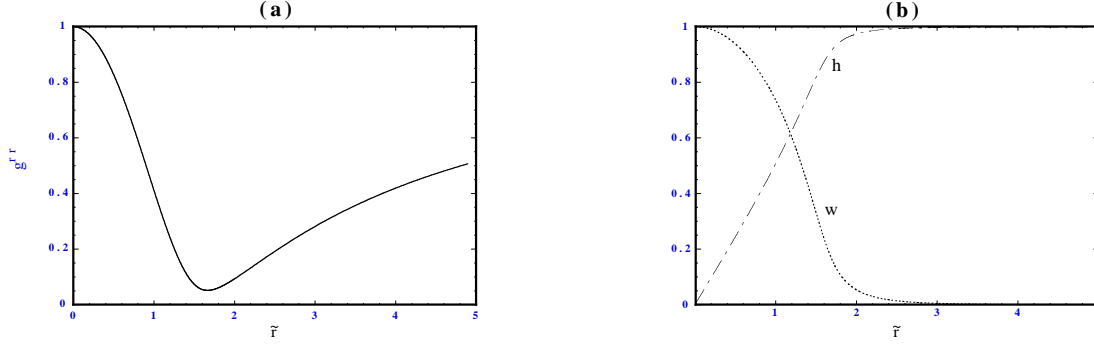


FIG. 3. Field configurations of the self-gravitating monopole with $\tilde{\lambda} = 0.2$ and $\omega = 0$ near the \tilde{v}_{max} ((a) $\tilde{r}-g^{rr}$ (b) $\tilde{r}-h, w$). Outside the minimum of g^{rr} , the solution can be approximated by RN black hole.

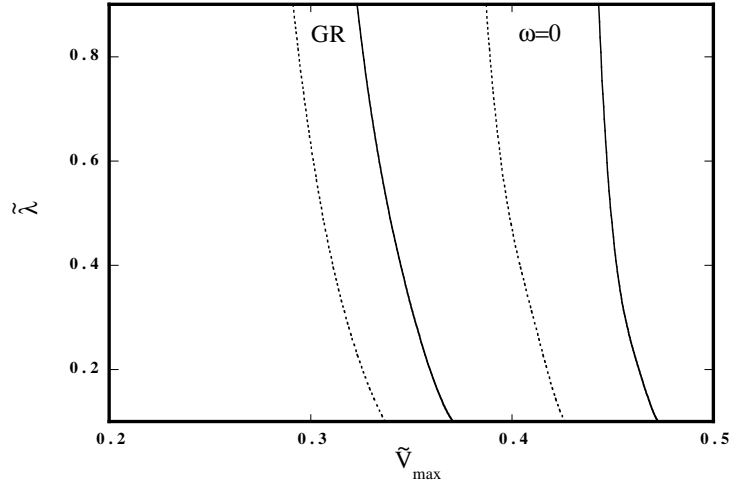


FIG. 4. The allowed region of the static solution for the self-gravitating monopole (the solid lines) and its black hole with $\tilde{r}_H = 0.4$ (the dotted lines). We compared these in the $\omega = 0$ and $\omega = \infty$ cases. Static solutions can exist to the left side of each line. For both solutions, \tilde{v}_{max} becomes large in BD theory. For the self-gravitating monopole, the nontrivial structure is larger than black hole's, so the change of \tilde{v}_{max} from GR becomes larger than its black hole's.

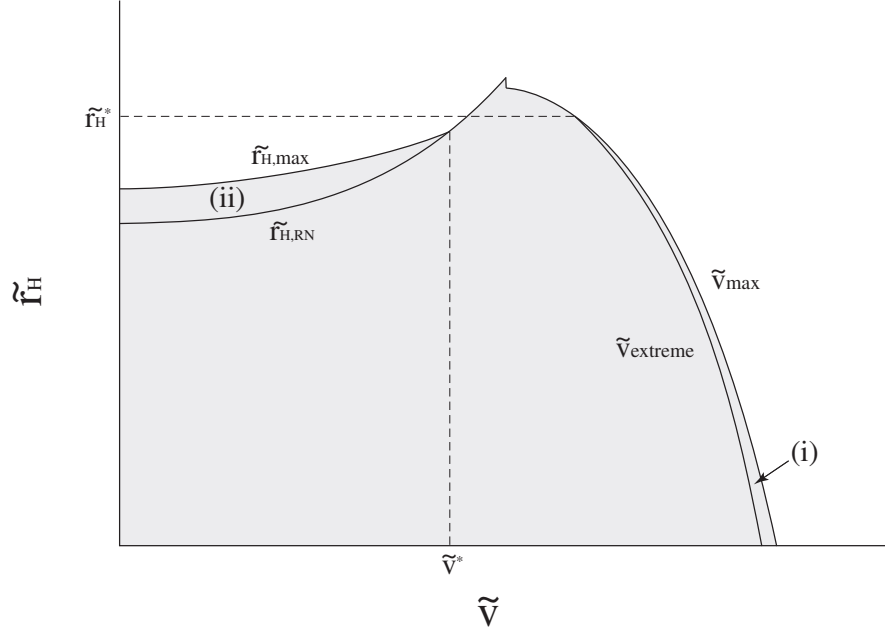


Fig.5

FIG. 5. Schematic diagram of the existence region in \tilde{v} - \tilde{r}_H diagram. In the shadowed region, the nontrivial solution exists. For a fixed value of $\tilde{r}_H < \tilde{r}_H^*$, there exists the region (i) ($\tilde{v}_{extreme} < \tilde{v} < \tilde{v}_{max}$) where two nontrivial solutions with different mass exist. On the other hand, for a fixed value of $\tilde{v} < \tilde{v}^*$, there exists the region (ii) ($\tilde{r}_{H,RN} < \tilde{r} < \tilde{r}_{H,max}$) where two nontrivial solutions with different mass exist. The region (i) and (ii) disappears for $\tilde{\lambda} > 0.287$ and $\tilde{\lambda} > 0.696$, respectively.

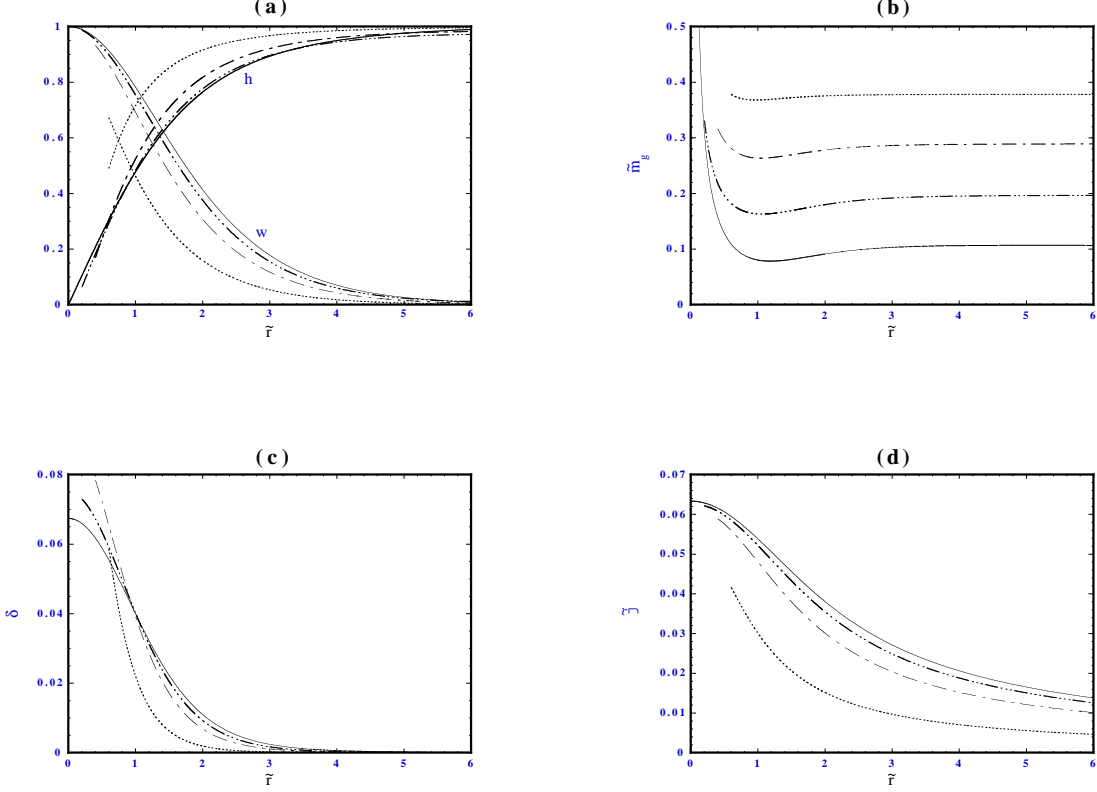


FIG. 6. Field configurations of the monopole black hole for $\tilde{\lambda} = 0.1$, $\tilde{v} = 0.1$, $\omega = 0$ and the horizon radius $\tilde{r}_H = 0.2, 0.4, 0.6$ ((a) $\tilde{r}-h$, w (b) $\tilde{r}-\tilde{m}_g$ (c) $\tilde{r}-\delta$ (d) $\tilde{r}-\tilde{\varphi}$). We also plot the self-gravitating monopole in the solid line (i.e., $\tilde{r}_H = 0$) for comparison. As the horizon radius becomes large, the nontrivial structure becomes small. So the variation of the BD scalar field becomes small.

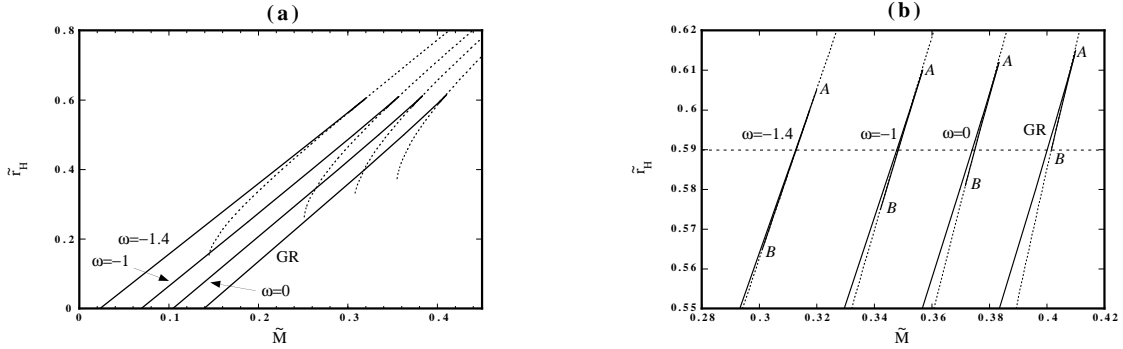


FIG. 7. Mass-horizon radius diagram of the monopole black hole for $\tilde{v} = 0.1$, $\tilde{\lambda} = 0.1$ and $\omega = -1.4, -1, 0, \infty$. ((b) is a magnification of (a) around the maximum horizon radius.) The solid lines denote monopole black holes and the dotted lines denote RN black holes. Unlike the RN black hole, the monopole black hole does not have an extreme limit but has the $\tilde{r}_H = 0$ limit, which corresponds to the self-gravitating monopole solution. The high entropy branch ends up with the maximum horizon radius and the maximum mass at point A, where a cusp structure appears. The low entropy branch is connected to the RN black hole branch.

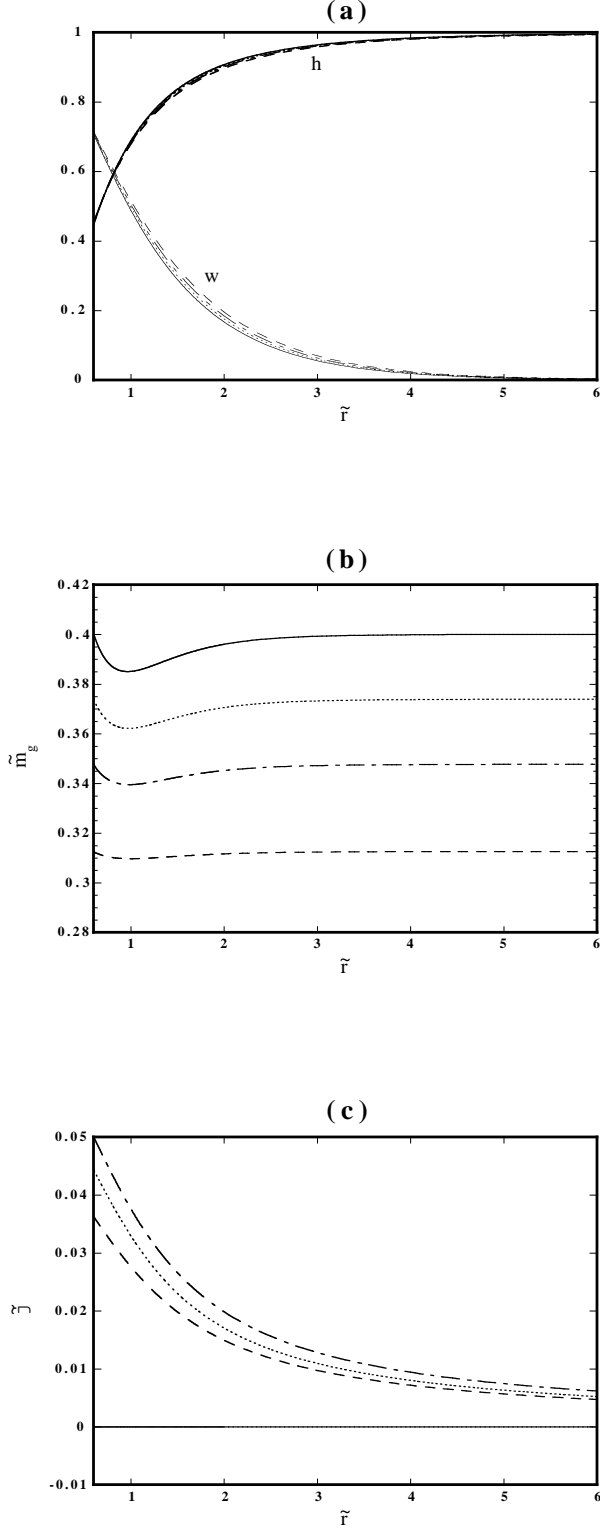


FIG. 8. Field configurations of the solution in the high entropy branch for $\tilde{r}_H = 0.59$, $\tilde{\lambda} = 0.1$, $\tilde{v} = 0.1$ and $\omega = -1.4, -1, 0, \infty$ ((a) $\tilde{r}-h, w$ (b) $\tilde{r}-\tilde{m}_g$ (c) $\tilde{r}-\tilde{\varphi}$). The YM field and the Higgs field hardly depend on ω .

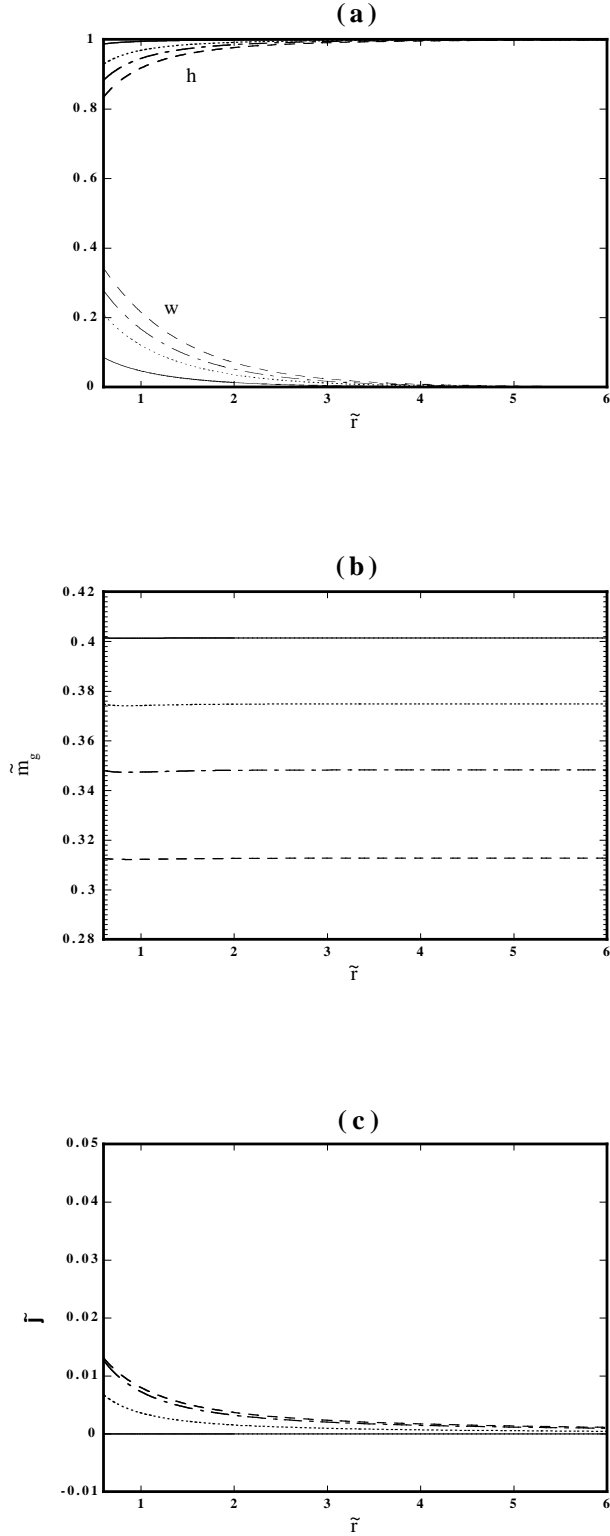


FIG. 9. Field configurations of the solution in the low entropy branch for $\tilde{r}_H = 0.59$, $\tilde{\lambda} = 0.1$, $\tilde{v} = 0.1$ and $\omega = -1.4, -1, 0, \infty$ ((a) \tilde{r} - h , w (b) \tilde{r} - \tilde{m}_g (c) \tilde{r} - $\tilde{\varphi}$). The YM field and the Higgs field depend on ω contrary to the high entropy branch. It is because $\tilde{r}_H = 0.59$ line crosses near the point A for small ω , but it crosses near the point B for large ω .

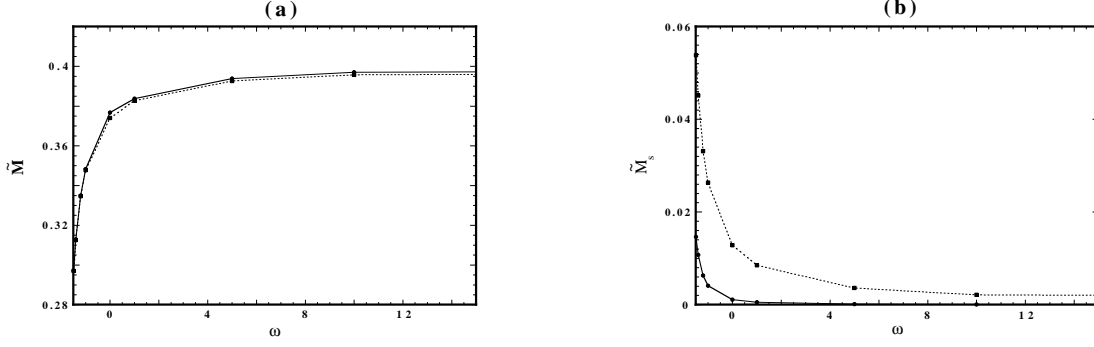


FIG. 10. ω dependence of (a) the gravitational mass and (b) the scalar mass of the monopole black hole for $\tilde{v} = 0.1$ and $\tilde{\lambda} = 0.1$. We choose $\tilde{r}_H = 0.59$ for which there exist two branches of monopole black holes for fixed ω . Though dependence of \tilde{M} in both branches can be approximated by a RN black hole, the effect of the nontrivial structure appears clearly for \tilde{M}_s .

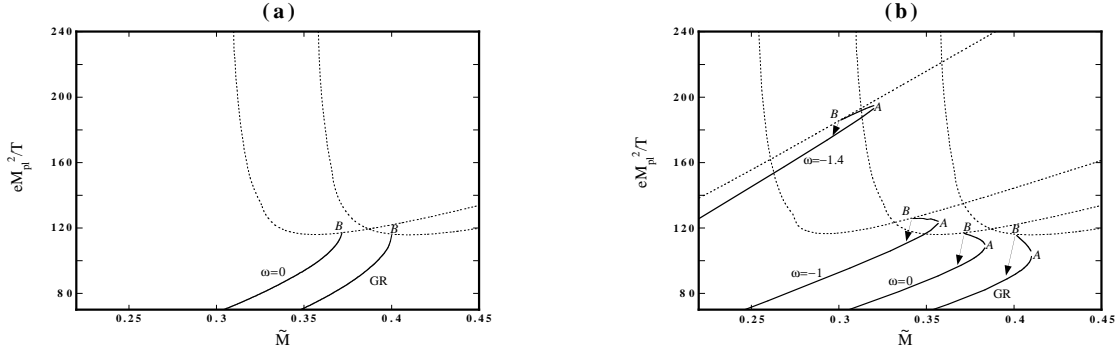


FIG. 11. Mass-inverse temperature diagram for (a) $\tilde{v} = 0.1$, $\tilde{\lambda} = 1$ and $\omega = 0, \infty$, (b) $\tilde{v} = 0.1$, $\tilde{\lambda} = 0.1$ and $\omega = -1.4, -1, 0, \infty$. When we consider the Hawking evaporation of a RN black hole, the solution experiences the second order phase transition for $\tilde{\lambda} = 1$ when the solution changes to the monopole black hole at the point B . On the contrary, it experiences first order phase transition for $\tilde{\lambda} = 0.1$.

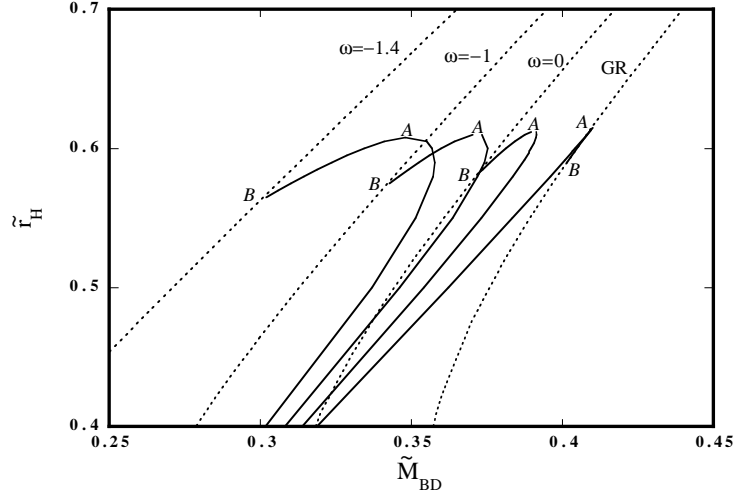


FIG. 12. Gravitational mass-horizon radius diagram of the monopole black hole in BD frame for $\tilde{v} = 0.1$, $\tilde{\lambda} = 0.1$ and $\omega = -1.4, -1, 0, \infty$. The solid lines denote the monopole black hole and the dotted lines denote the RN black hole. In this diagram, a cusp structure disappears. This may show that \tilde{M}_{BD} is not appropriate to the control parameter of catastrophe theory.